C. R. Physique 3 (2002) 141–151

Physique statistique, thermodynamique/*Statistical physics, thermodynamics*
(Solides, fluides : propriétés mécaniques et thermiques/*Solids, fluids: mechanical and thermal properties*)

DOSSIER

PHYSIQUE DE LA MATIÈRE EN GRAINS
PHYSICS OF GRANULAR MEDIA

The stress response function in granular materials

Jean-Philippe Bouchaud [a]*, Philippe Claudin [b], Eric Clément [b], Matthias Otto [a], Guillaume Reydellet [b]

[a] **Service de physique de l'état condensé, CEA-Saclay, Orme des Merisiers, 91191 Gif-sur-Yvette cedex, France**

[b] **Laboratoire des milieux désordonnés et hétérogènes (UMR 7603 du CNRS), 4, place Jussieu, case 86, 75252 Paris cedex 05, France**

Received 21 September 2001; accepted 11 December 2001

Note presented by Guy Laval.

Abstract We discuss the relevance the study of the stress response function in granular materials, i.e. of the stress profile under a layer of grains submitted to a localized force at its top surface. We first present a quantitative comparison between the experimental measure of this function with isotropic elastic predictions. We then give a description in terms of a model of force chains. ***To cite this article: J.-P. Bouchaud et al., C. R. Physique 3 (2002) 141–151.*** © 2002 Académie des sciences/Éditions scientifiques et médicales Elsevier SAS

stress response / elasticity / force chains

Fonction de réponse dans les matériaux granulaires

Résumé Nous discutons l'intérêt de l'étude de la function de réponse dans les matériaux granulaires, c'est à dire du profil de pression sous une couche de grain soumise à une surcharge localisée à sa surface. Nous présentons d'abord une comparaison quantitative entre la mesure expérimentale de cette fonction avec les prédictions de la théorie élastique isotrope. Nous donnons ensuite une description en termes d'un modèle de chaînes de force. ***Pour citer cet article : J.-P. Bouchaud et al., C. R. Physique 3 (2002) 141–151.*** © 2002 Académie des sciences/Éditions scientifiques et médicales Elsevier SAS

réponse en contrainte / élasticité / chaînes des force

1. Introduction

The pressure underneath a conical sandpile created by pouring hard, cohesionless grains from a point source, exhibits a central 'dip' (i.e. a pressure minimum) underneath the point where the height of the pile is maximum. This surprising result, reported by Šmíd and Novosad in 1981 [1], has now been unambiguously reproduced by many groups [2]. This effect is not an artefact (caused, for example, by the precise properties

* Correspondence and reprints.
E-mail addresses: bouchard@spec.saclay.cea.fr (J.-P. Bouchaud); claudin@ccr.jussieu.fr (P. Claudin); erc@ccr.jussieu.fr (E. Clément); reydelle@ccr.jussieu.fr (G. Reydellet).

S1631-0705(02)01307-5/FLA

of the base, as was suggested in [3]). It is demonstrated by the fact that for the very same grains but a different creation history where the pile is built layer by layer, the dip disappears and is replaced by a broad central hump [4].

This now famous example shows that the statics of granular matter is a rather non trivial problem where history or sample preparation is extremely important (see, e.g., [5–7]). A rather striking feature of granular systems is the presence of force chains [8,9]. It was shown in particular that the set of 'large' inter-particle forces forms a cell like structure of size on the order of 10 particle diameters for disordered packing. This structure evolves in response to external sollicitations [10,11] and its geometrical characteristics—the so-called internal texture of the granular medium [12]—reflects the past history of the system. Smaller forces, present with a significant probability [12,13], stabilize larger force chains against buckling but show no specific structure and are more randomly distributed.

How can one then describe the statics of granular materials on large length scales? The standard way to approach the problem is to use elasto-plastic theories from soil mechanics [14]. However, the relation between force chains on short length scales and an elasto-plastic description on large length scales is far from obvious. There are also some conceptual problems: even if an elastic-like description of small perturbations around an arbitrary reference state, such as sound waves, for example, might make sense in general (but see below), the description of, say, a conical sandpile using elasticity theory requires the identification of a (zero stress for example) reference state from which deformations can be defined. In the case of a pile of hard grains, with a Young modulus much larger than the gravity induced stresses, which rests in one particular metastable state (among a large number of macroscopically equivalent ones), switching the gravity back to zero will hardly affect the packing. Each of these metastable states could thus equally well be taken as a reference state.

Even the description of small perturbation might be problematic. For example, the existence of a (large volume) limiting curve relating incremental stresses and deformations requires at least some 'annealing' procedure (slow compaction) to define a reproducible initial state. Note that this limiting curve might not even exist in the absence of friction [15] and that even for moderate deformations, following the so-called consolidation phase, the response to cyclic loads in standard triaxial tests shows some significant irreversibility.

The absence of any obvious deformation field from which the stress tensor may be constructed has motivated an alternative, 'stress-only' approach [16–20]. The basic tenet of these theories is that in equilibrium, some history dependent large scale statistical relations between the components of the stress tensor are established. These relations should only depend on some global statistical features of the particular metastable state in which the packing sits but not on its microscopic details. A well-known relation of this type arises from the assumption that the material is on the verge of plastic failure, leading to a Mohr–Coulomb (nonlinear) relation between the stress components [21]. A simpler relation, based both on symmetry arguments [16] and on the consideration of simple rules for the transfer of stresses between adjacent grains [22], is a local proportionality between the diagonal components of the stress tensor. For example, in two dimensions, this relation can be expressed as $\sigma_{zz} = c_0^2 \sigma_{xx}$, where c_0 is a constant. This equation is actually a local version of the hypothesis made by Janssen in his famous theory for stresses in silos [20,21,23]. The consequence of this apparently innocuous assumption is that stresses obey a 'hyperbolic' equation, as compared to the elliptic equations encountered in elasticity theory. This means that stresses 'propagate' or are 'transmitted' along lines: the characteristics of this hyperbolic equation were argued to be the mathematical transcription of the 'force chains' that are well known to exist in granular materials [24]. More elaborated versions of the above closure relation between the components of the stress tensor have been investigated in [17,18,20], which can be seen as anisotropic generalisations of the Mohr–Coulomb relation that accounts for the texture of the material [20]. The parameters appearing in these closure schemes can be chosen as to reproduce both the pressure 'dip' underneath the apex of a sandpile [1,2,4], or the pressure profile inside silos [23]. Finally, isostatic assemblies of grains [25,26] have been argued to exhibit at large scales such relations between stress components [27,28], in particular when

composed of frictionless beads [29,30] for which the simple rules for stress transfer mentioned above can be justified.

A rather clear-cut difference between hyperbolic and elliptic equations lies in the structure of the propagator, i.e. the response of the stress field to a localized force applied at the top of a layer of granular matter of height h. For a hyperbolic equation, the pressure profile at the bottom of the layer is localized around two peaks (in two dimensions) or three peaks or a circular annulus (in three dimensions, depending on the symmetry), centred underneath the point where the force is applied [16]. For an elliptic equation, by contrast, the response function is a bell shaped curve of width proportional to h that reaches its maximum precisely underneath the point where the force is applied. A similar single peak structure, but of width proportional to $\sqrt{h}$, is also predicted by scalar models [31,32], where the stress obeys a (parabolic) diffusion equation. In view of its importance, there has recently been a significant effort to gather experimental, numerical and theoretical results on this question. In this paper, we review some progress concerning the experimental determination of the response function and in particular, we focus on the results obtained in [33], that favor an elliptic-like response for strongly disordered packings at large scale. Then, we discuss a recently proposed theoretical model which builds upon the original hyperbolic models, where strong disorder leads to force chain splitting and merging. This mechanism strongly randomizes the local direction of stress propagation, and transforms a locally hyperbolic behaviour (encoding the existence of force chains) into a large scale pseudo-elastic behaviour without the introduction of any deformation field. Finally, we discuss the future directions we seek to pursue, both experimentally and theoretically, in an effort to clarify the mechanical status of granular packings.

2. Experimental determination of the response function

The stress 'response function' to a localized overload is of prime interest both from a fundamental point of view but also for many engineering applications. On large scales, the extra stresses created by a house within the soil beneath it are indeed related to this response function. Therefore, this problem has received considerable theoretical attention in the engineering community, where, as mentioned above, the granular material is often assumed to be a (possibly anisotropic) elastic material. Note that an elliptic response function corresponds to a favorable case for stability since the stresses are efficiently dispersed in space, whereas a hyperbolic response function would lead to a rather localized stress field.

In spite of its importance, the response function of granular assemblies has only very recently been measured experimentally [33–35]—see Fig. 1. Various methods were used: one is a direct quantitative measurement of the response at the bottom of 3D packing using a local stress probe based on the deformation of a hard membrane [33], another method is based on carbon paper imprints created by a monodisperse 3D packing [35]. For 2D packing the photoelastic response of polymeric grains was used [34] in order to evidence the inter-particle force path. This is a semi-quantitative method but it allows the visualization directly of the response in the bulk as well as the topology of the path followed the stress chains. Such an observation will be used to built the theoretical proposition exposed in the following chapter. These experimental efforts have lead so far to the following picture (note however that a purely 'diffusive' response function, scaling as $\sqrt{h}$, was reported in [36] for a very special 'brick' packing): for

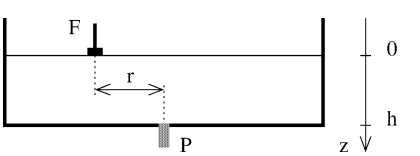

Figure 1. Sketch of the experimental set-up used in [33,43,45]. A localized vertical force F is applied on the top surface of the granular layer ($z = 0$). The corresponding vertical pressure response P on the bottom is measured at some distance r from that point from a tiny change of the electrical capacitance of the probe when its top membrane is slightly deformed. The vertical z-axis points downwards and we note h the thickness of the layer (between 0 and 10 cm). Natural 'Fontainebleau' sand whose typical diameter is ~ 0.3 mm was used.

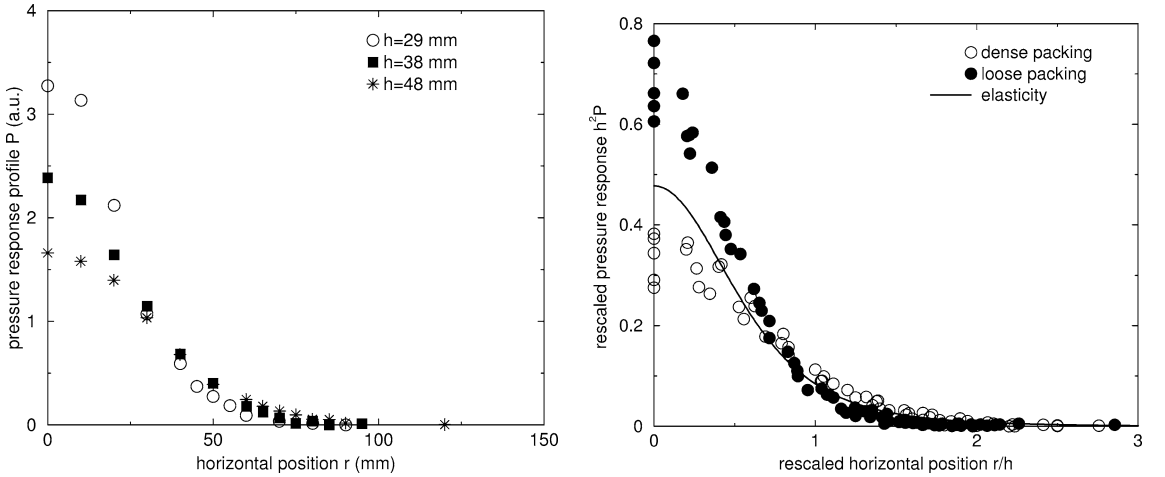

Figure 2. Left: dense pressure profiles $P(r)$ for three different values of the thickness h. Right: pressure profiles rescaled by h. This plot shows that the pressure response depends on the way the system of grains was prepared: it is broader for a dense packing (empty circles) than for a loose one (filled circles). The response of a semi-infinite isotropic elastic medium (solid line) lies in between the two. From [43].

strongly disordered packings, for example by considering mixtures of grains of very different sizes, or irregular grains such as natural sand, the response profile on large length scales shows a single broad peak [33,34]. This single hump response function was also observed in numerical simulation of 2D polygonal grains packing [37].

For well-ordered packings however, the two peaks structure is rather convincingly observed two dimensions (a 'ring' or three peaks in 3D) [34,35,38]. These hyperbolic features are also in agreement with a recent numerical simulation on (rather small) isostatic assemblies of frictionless grains [29,30,39] (although the large scale limit might be elliptic [25]), with the work reported in [40,41] where beads are arranged on a regular triangular lattice but where disorder is introduced by a finite friction coefficient and also, for strongly anisotropic elastic networks at small length scales [42].

Obtaining a precise experimental determination of the linear response function that can be quantitatively compared to theoretical models is rather difficult: the perturbation must be small enough not to disrupt the packing, but also large enough to lead to a measurable signal. A very sensitive technique, based on a lock-in detection of an oscillating perturbation, has allowed one to obtain precise and reproducible results [33,43]; these are shown in Fig. 2 (left) for (dense) layers of sand of different heights.

One finds unambiguously that the response function $G(r,h)$ to a perturbation located at $r_0 = z_0 = 0$ is in this case single-peaked, with a width growing as the height h of the layer. More precisely, the response function for different heights can be rescaled onto a unique curve by plotting $h^2 G(r,h)$ as a function of r/h, see Fig. 2 (right). The factor h^2 is expected from force conservation: the integral of the response function over the bottom plate must be equal to the overload force F for the total force to balance. Note that due to screening effects (arching) around the probe, this integral, computed from the experimental data actually shows a large dispersion from one experiment to another and is on average less than F ($\sim 80\%$). This screening effect is well known to be inherent to every mesurement of stresses in granular materials [3], but we corrected for this effect by using the measured integral F^* to rescale the pressure measurements: $P \leftarrow P/F^*$. Very importantly, it was also checked that the response is linear for the range of applied forces used.

Fig. 2 (right) shows also that, like for the sandpile, the pressure response profile depends on the way the granular layer was prepared—its 'history': the value of the maximum of this response is roughly twice smaller (and its width twice larger) for a dense packing than for a loose one. In Fig. 3, we compare

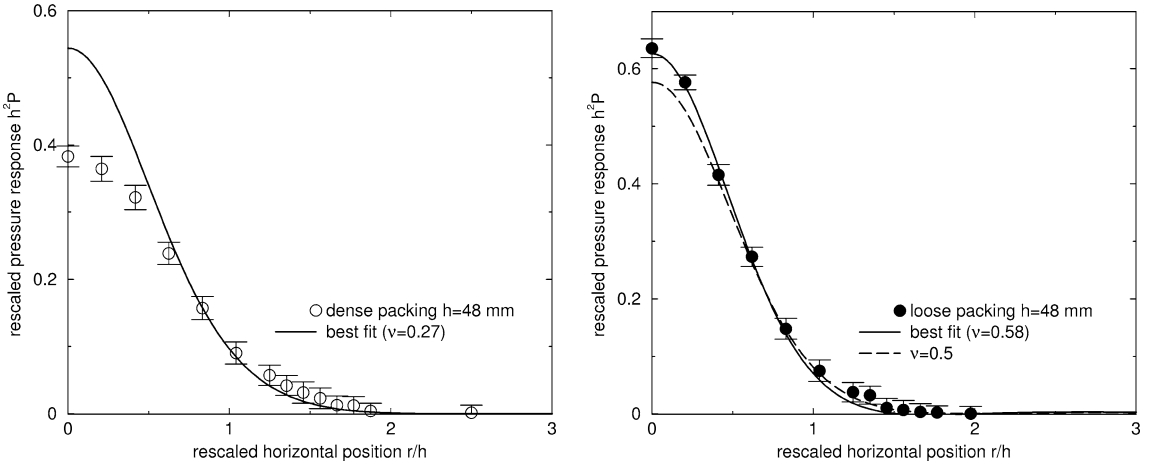

Figure 3. Left: fit of the dense packing data. The agreement is not good at all (the corresponding Poisson coefficient is therefore not meaningful). Right: fit of the loose packing data. The best fit value for ν exceeds the elastic bound $\nu \leqslant 1/2$. From [43].

the shape of the scaling function obtained for these two different preparations of the sand layer—loose packing or dense packing—to the prediction of elasticity theory. Assuming a simple isotropic elasticity and a rough bottom plate leaves us with a single adjustable parameter, namely the Poisson coefficient ν (the Young modulus does not appear in the response function). As shown in Fig. 3, the quantitative shape of the experimental response function cannot be accounted for: for the dense layer, the best fit is very bad, whereas for a loose layer the fit is acceptable, but leads to a Poisson coefficient $\nu \simeq 0.6$ that violates the bound $\nu \leqslant 1/2$—see [43] for more details on the fitting procedure as well as the elastic calculation. It is however known that extending elasticity theory to non isotropic materials provides additional elasticity constants that can strongly affect the shape of the response function [42,44]. In the present case, we expect isotropy in the plane perpendicular to h, which leads to three extra adimensional constants that can be adjusted. Work is underway to fit the experimental results within this extended framework (see also the discussion below).

So far, we have discussed packing that is locally isotropic in the plane perpendicular to h, and therefore leads to a response function that is symmetric: $G(r,h) = G(-r,h)$. Correspondingly, for a sandpile constructed in a similar way, i.e. layer by layer, no pressure dip is observed. It is interesting to study the response function in a layer which has an anistropic texture. This can be realized by either shearing the layer, or by constructing it by successive avalanches from (say) left to right and break the axial symmetry.

One can also measure directly the response function underneath a sandpile created from a point source, where the perturbation is applied at the apex of the pile. These experimental verifications which aim is to clarify the role of the texture and its consequence at a macroscopic level are in progress.

3. The λY force splitting model

3.1. Introduction and numerical simulation

From pictures of photoelastic grains, the network of interparticle forces propagating as a responses to a localized pressure was extracted [34,45] (see Fig. 4). An interpretation of such a picture can be given in terms of linear force chains which tend to split upon meeting vacancies or packing defects [46].

The role of disorder on hyperbolic equations was previously investigated in [22], where the constant c_0 in the equation relating σ_{zz} and σ_{xx} was allowed to be randomly fluctuating in space. The study was restricted to small fluctuations (i.e. $c_0(\vec{r}) = \bar{c}_0 + \delta c(\vec{r})$, with $\delta c \ll \bar{c}_0$), where perturbation theory is valid.

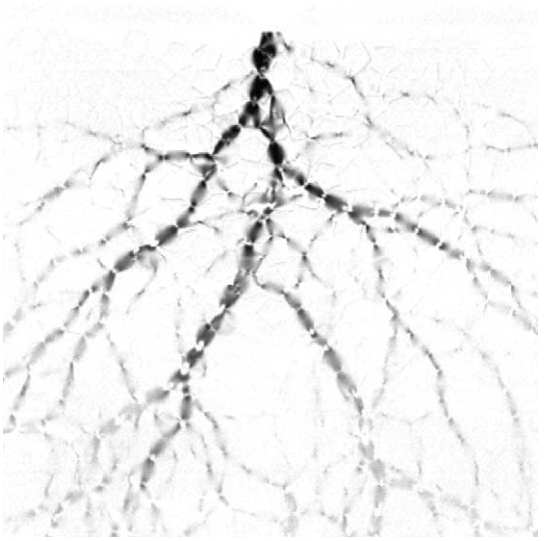

Figure 4. Picture of the response force chains in a two-dimensional system of grains subject to a vertical force imposed at the middle of the top surface. To get this picture birefringent grains between inverse circular polarizers have been used, and the intensity difference after and before the overloading has been computed. This picture is from R.P. Behringer and J. Geng.

In this case, the two peak structure of the response function is preserved on large length scales, although the peaks are diffusively broadened. This result is in qualitative agreement with the numerical simulations [39–41]. An uncontroled extrapolation to strong disorder, however, suggested that the large scale equations might become elliptic.

In order to investigate more quantitatively the strongly disordered regime where force chains split and merge, we have studied in [46] the following model. If one of the force chains meets a defect (randomly distributed in space), we split it into two new ones at a random angle, which then propagate until another defect (or the boundary) is reached. More precisely, a chain carrying a force f in the direction $\vec{n}$ splits when meeting a defect into two forces f_1, f_2 in the directions $\vec{n}_1$, $\vec{n}_2$—'λ process'. The two angles θ_1 and θ_2 (between $\vec{n}, \vec{n}_1$ and $\vec{n}_1, \vec{n}_2$, respectively) are uniformly chosen between 0 and some maximum splitting angle θ_{M}. The local mechanical equilibrium imposes that the intensities f_1 and f_2 are such that $f\vec{n} = f_1\vec{n}_1 + f_2\vec{n}_2$. Sometimes, two (or more) force chains meet at the same defect—'Υ process'. In this case, we make them merge together. It is important to note that the positions of the defects are fixed before starting the computation of the forces. This idea of a frozen disorder is consistent with the experimental observation that when the local overload is added on the top of the system, the forces are transmitted along the chains originally created during the building of the packing. In other words, as long as the applied force is not too large and compatible with the pre-existing network of force chains, the geometry of the packing, and in particular the contacts between grains, remains the same.

With these rules, realistic force networks can be created—see Fig. 5. After averaging over many statistically identical samples, one can obtain stress profiles for different heights h.

Fig. 6 shows that, as h increases, the vertical pressure response profile evolves continuously from two well defined peaks to a single broad one. It means that the hyperbolic behaviour is progressively erased by multiple scattering. The width of the single peak is found to scale scales like h; the scaling function is furthermore surprisingly close to the pure elastic response of a semi-infinite two-dimensional medium, which becomes [47,48]:

$$G_{2\mathrm{D}}(x,h) = \frac{2}{\pi h}\,\frac{1}{[1+(x/h)^2]^2}. \tag{1}$$

Note, however, that some force chains are deflected upwards and reach the top of the system. The top layer only remains stable as long as these forces do not exceed the weight of a single grain. For larger applied forces, one expects the top layer to become unstable.

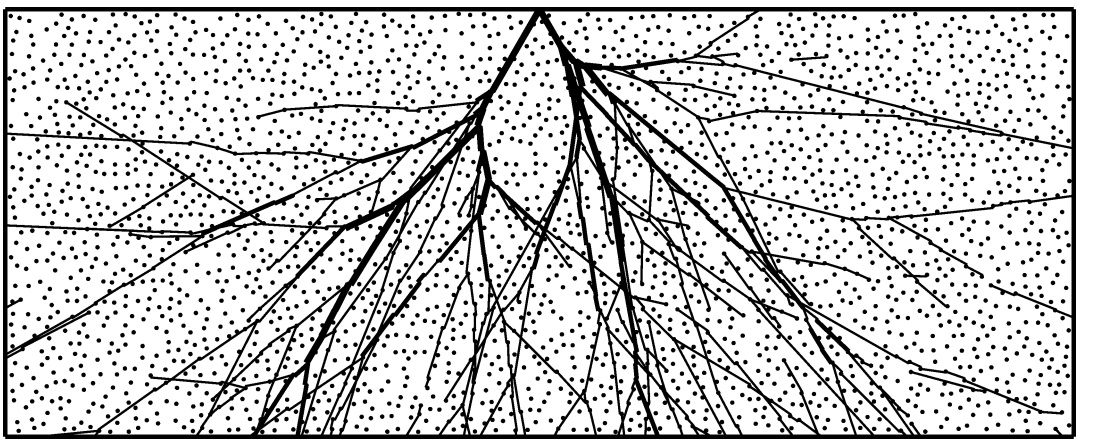

Figure 5. Snapshot of the network of force chains obtained within the λ Υ model. The dots represent the defects of the granular packing. The lines are bolder when the forces are larger—very small forces (less than 0.01) have not been plotted. In this picture we set the height to $h = 200$, the width to $2w = 500$, the density of defects to $\rho_{\mathrm{d}} = 0.028$ and the maximum splitting angle to $\theta_{\mathrm{M}} = 30^{\circ}$.

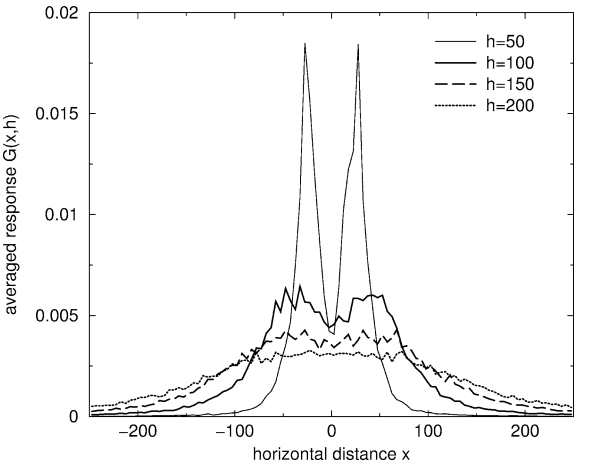

Figure 6. Averaged vertical stress response function for different values of h. At small scale, the response function has a double peak shape which is characteristic of a locally hyperbolic behaviour. For larger heights, these two peaks merge into a single broad peak, comparable to an elastic-like response. These curves have been obtained with $2w = 500$, $\rho_{\mathrm{d}} = 0.028$, $\theta_{\mathrm{M}} = 30^{\circ}$, and averaged over 1000 samples.

3.2. A Boltzmann description of force chain splitting

In order to understand analytically the above numerical results, we write a Boltzmann equation for the probability density $P(f, \vec{n}, \vec{r})$ of finding an oriented force chain of intensity f in the direction $\vec{n}$ around the point $\vec{r}$ [46]. A very important point here is that force chains can be oriented in reference to the boundary conditions (see the discussion in [29,30,49]).

For simplicity, we neglect the chain 'merging' process which leads to a more complicated nonlinear Boltzmann equation (its influence will be discussed in a forthcoming work [52,53]). We also assume that the splitting is symmetric, i.e. that $\vec{n} \cdot \vec{n}_1 = \vec{n} \cdot \vec{n}_2 \equiv \cos\theta$, so that $f_1 = f_2 = f/2\cos\theta$. Assuming a uniform density of defects, the probability distribution $P(f, \vec{n}, \vec{r})$ obeys the following general equation:

$$P(f, \vec{n}, \vec{r} + \vec{n}\,\mathrm{d}r) = \left(1 - \frac{\mathrm{d}r}{\lambda}\right) P(f, \vec{n}, \vec{r}) + 2\frac{\mathrm{d}r}{\lambda} \int \mathrm{d}\vec{n}' \int \mathrm{d}f' P(f', \vec{n}', \vec{r}\,) \Psi(\vec{n}', \vec{n}) \delta\left(f - \frac{f'}{2\cos\theta}\right), \quad (2)$$

where λ is equal to the 'mean free path' of force chains, and is of order $1/(\rho_{\rm d} a^{D-1})$ in dimension D. The above equation means the following: since a chain of grains can only transport a force parallel to itself [24], the direction of the force $\vec{n}$ also gives the local direction of the chain. Between $\vec{r}$ and $\vec{r} + \vec{n}\,{\rm d}r$, the chain can either carry on undisturbed, or be scattered. The second term on the right hand side therefore gives the probability that a force chain initially in direction $\vec{n}'$ is scattered in direction $\vec{n}$. This occurs with a probability $\frac{{\rm d}r}{\lambda}\Psi(\vec{n}', \vec{n})$, where Ψ is the scattering cross section, which we will assume to depend only on the scattering angle θ, for example a uniform distribution between $-\theta_{\rm M}$ and $+\theta_{\rm M}$. The δ-function ensures force conservation and the factor two comes from the counting of the two possible outgoing force chains. Let us now multiply Eq. (2) by f and integrate over f. This leads to an equation for the local average force per unit volume in the direction $\vec{n}$, that we will denote $F(\vec{n}, \vec{r})$. This equation reads:

$$\lambda \vec{n} \cdot \vec{\nabla}_r F(\vec{n}, \vec{r}) = -F(\vec{n}, \vec{r}) + \int {\rm d}\vec{n}' \frac{F(\vec{n}', \vec{r})}{\vec{n} \cdot \vec{n}'} \Psi(\vec{n}', \vec{n}) + \frac{\lambda}{a} \vec{n} \cdot \vec{F}_0(\vec{r}), \tag{3}$$

where we have added the contribution of an external body force density $\vec{F}_0(\vec{r})$, and a is the size of a defect or of a grain. This equation is the so-called Schwarschild–Milne equation for radiative transfer, decribing the evolution of light intensity in a turbid medium [50]. We now introduce some angular averages of $F(\vec{n}, \vec{r})$ that have an immediate physical interpretation:

$$p(\vec{r}) = a \int {\rm d}\Omega\, F(\vec{n}, \vec{r}) \tag{4}$$

$$J_\alpha(\vec{r}) = a \int {\rm d}\Omega\, n_\alpha F(\vec{n}, \vec{r}) \tag{5}$$

$$\sigma_{\alpha\beta}(\vec{r}) = a D \int {\rm d}\Omega\, n_\alpha n_\beta F(\vec{n}, \vec{r}), \tag{6}$$

where $\int {\rm d}\Omega$ is the normalized integral over the unit sphere, that is introduced for a correct interpretation of σ (see Eq. (10) below). As will be clear from the following, $\vec{J}$ is the local average force chain intensity per unit surface, σ is the stress tensor. Since $\vec{n}^2 = 1$, one finds that ${\rm Tr}\,\sigma = Dp$, and therefore p is the isostatic pressure. Note that $\vec{J}$ is not the average local force, which is always zero in equilibrium. The fact that $\vec{J} \neq \vec{0}$ comes from the possibility of 'orienting' the force chains.

We now integrate over the unit sphere Eq. (3) after multiplying it by different powers of n_α. Using the fact that $\Psi(\vec{n}', \vec{n})$ only depends on $\vec{n} \cdot \vec{n}'$, a direct integration leads to:

$$\lambda \vec{\nabla} \cdot \vec{J} = (a_0 - 1)\, p, \tag{7}$$

where a_0 is called the 'albedo' in the context of light scattering [50], and can be written:

$$a_0 \equiv \int {\rm d}\vec{n} \frac{\Psi(\vec{n}', \vec{n})}{\vec{n} \cdot \vec{n}'} \geqslant 1. \tag{8}$$

A second set of equations can be obtained by multiplying by n_α and integrating. Using the fact that $\int {\rm d}\vec{n}\, \Psi(\vec{n}', \vec{n}) = 1$, it is easy to show that

$$\int {\rm d}\vec{n}\, \vec{n} \frac{\Psi(\vec{n}', \vec{n})}{\vec{n} \cdot \vec{n}'} = \vec{n}'. \tag{9}$$

Therefore, the resulting equation is nothing but the usual mechanical equilibrium relation:

$$\nabla_\beta \sigma_{\alpha\beta} = F_{0\alpha}. \tag{10}$$

This relation reflects the local balance of forces chains. Now we multiply Eq. (3) by $n_\alpha n_\beta$ and again integrate. A priori, this introduces a new three index tensor. In order to close the equation, we now make the an assumption that is usually made in the context of light diffusion, that on large scales the force intensity becomes nearly isotropic [50]. In this case, it is justified to expand $F(\vec{n}, \vec{r})$ in angular harmonics and to keep only the first terms:

$$a\, F(\vec{n}, \vec{r}) = p(\vec{r}) + D\vec{n} \cdot \vec{J}(\vec{r}) + \cdots. \tag{11}$$

Within this expansion, we finally obtain a 'constitutive' relation between $\sigma_{\alpha\beta}$ and the vector $\vec{J}$. We find:

$$\sigma_{\alpha\beta}\big|_{\alpha\neq\beta} = \frac{\lambda D^2 K_1}{\left(\frac{Da_2 - a_0}{D-1} - 1\right)}(\nabla_\alpha J_\beta + \nabla_\beta J_\alpha) \quad \text{and} \tag{12}$$

$$\sigma_{\alpha\alpha} = \frac{\lambda D}{\left(\frac{Da_2 - a_0}{D-1} - 1\right)}\left[2DK_1 \nabla_\alpha J_\alpha + \left(DK_1 - \frac{a_0 - a_2}{(D-1)(a_0-1)}\right)\vec{\nabla}\cdot\vec{J}\right], \tag{13}$$

with $K_1 = 1/D(2+D)$ and $a_2 = \int \mathrm{d}\vec{n}\,(\vec{n}\cdot\vec{n}')\Psi(\vec{n}', \vec{n})$. Rather surprisingly, these equations have exactly the canonical form of elasticity theory, provided one identifies the vector $\vec{J}$ with the local displacement, up to a multiplicative factor. The analogue of the Poisson ratio ν can be written:

$$\nu = \frac{1}{D-1}\,\frac{D - 1 + 3a_0 - (D+2)a_2}{D + 1 + a_0 - (D+2)a_2}. \tag{14}$$

Note that this quantity is purely geometric, and does not involve the scattering mean free path λ. Since $a_0 \geqslant 1$ and $a_2 \leqslant 1$, it is easy to show that $\nu \geqslant 1/(D-1)$ in all dimensions, therefore violating the thermodynamical bound $\nu \leqslant 1/(D-1)$ that holds for conventional elastic bodies. This means that the stress equations cannot be derived from the minimisation of a positive quadratic free energy functional, as is the case for standard elasticity.

The force chain splitting model in $D = 3$ is easily generalized from 2 to 3 outgoing force chains. Each direction $\mathbf{n}_i$, $i = 1, 2, 3$, is specified by spherical coordinates φ_i, θ_i. The constraints for the force balance are readily generalized within the Boltzmann equation. The analogue of symmetric splitting for two outgoing chains is that in a plane perpendicular to the incoming force chain, the outgoing chains will be points of an equilateral triangle. When drawing one direction from a uniform distribution, say φ_1 from $[0, 2\pi/3]$, and $\theta_1 \leqslant \theta_{\max} < \pi/2$, then the remaining direction will lie on the triangle with $\theta_2 = \theta_3 = \theta_1$. An explicit computation gives modified results for the constants a_0, a_1, a_2. However, the Poisson ratio as a function of $\theta_{\max}$ is very close to the curve found for two-chain splitting, and still violates the bound $\nu \leqslant 1/2$. We are currently studying the influence of the merging processes which might reduce the value of ν.

The above stress equations are rather nontrivial because no displacement field is introduced in the above derivation (nor in the numerical model): elastic-like equations are found in a stress-only model. The basic assumption is the existence of local force chains, which have a well defined identity over several grain sizes a, such that $a \ll \lambda$: this is the condition under which the above Boltzmann description of the force chain scattering is justified.

Since the above equations are formally identical to those of classical elasticity, one can show that $\nabla^2 p = 0$, and $\nabla^4 \vec{J} = 0$ [47]. One can therefore in principle compute the response function $G(\vec{r})$ to a localized force at $\vec{r}_0 = 0$ in the z direction, which is given in $2D$ by Eq. (1). Note, however, that although the above equations are formally those of classical elasticity, there is one crucial difference coming from the fact that $(\sigma_{\alpha\beta})$ and $\vec{J}$ are not independent since they are both related to the same underlying quantity $F(\vec{n}, \vec{r})$. This is a very important difference, which is appears in the choice of boundary conditions on $\mathcal{B}$ which determines $P(f, \vec{n}, \vec{r})|_{\mathcal{B}}$.

4. Conclusion and open problems

In this paper, we have reviewed recent experimental results which strongly suggest that for disordered packings, the response function is in qualitative agreement with the prediction of an elliptic (elastic-like) theory, and in conflict with the prediction of the family of hyperbolic models put forward in [16–20]. Although the perturbative calculation of [22] suggests that the localized nature of the response function survives to weak disorder (and could explain the experimental results on well ordered packings and the numerical results of [29,30,39–41]), we present a recent calculation [46] showing that in the presence of a strong disorder that 'scatters' the force chain the local hyperbolic character of the stress equations is unstable at large length scales. The effective large scale equation that are obtained from a Boltzmann-like description of the force chain splitting are akin to those of a conventional elastic body (although the boundary conditions are different). There are two main advantages in this new approach. First, no real displacement field is needed, and second, it allows us to calculate the pseudo-elastic coefficients from microscopic geometrical quantities—the force chains angular distribution.

However, the calculations discussed above are restricted to an isotropic situation where the scattering function $\Psi(\vec{n},\vec{n}')$ only depends on $\vec{n}\cdot\vec{n}'$. This leads, not surprisingly, to an isotropic elasticity like equations which are, as emphasized above, unable to describe quantitatively the shape of the experimental response function. These isotropic equations, obviously, cannot reproduce the pressure dip in the sandpile either. An important problem is then to generalize the above theory to take into account nonisotropic scattering functions, that could depend not only on $\vec{n}\cdot\vec{n}'$ but also on $\vec{N}\cdot\vec{n}'$, where $\vec{N}$ is a (space-dependent) vector that describes the local texture, i.e. the nonisotropic distribution of contacts between grains. In this case, combinations like $N_\alpha N_\beta$ can appear in the stress tensor $\sigma_{\alpha\beta}$. The vector $\vec{N}$ is expected to encode the construction history of the material, and should be non trivial, for example, in a sandpile constructed from a point source [51], or for layers under shear. In the presence of a long-ranged texture field $\vec{N}$, the resulting equations are similar to those of anisotropic elasticity theory, and are currently under scrutiny [52]. The comparison of this extended theory with the experimental results, both on the response function and for the sandpile problem, would be very instructive, and give in particular information on the local structure of the packing.

Finally, let us note that the local fluctuations of stresses in granular materials are very important and have been much discussed recently [31,32]. The above theoretical framework should allow to make some progress, by studying higher moments of the local force distribution $P(f,\vec{n},\vec{r})$, beyond the average force $F(\vec{n},\vec{r})$ studied here. For these quantities, the role of merging processes is probably very important.

Acknowledgements. Part of this work is the result of a very stimulating collaboration with R.P. Behringer, D. Levine, J. Geng, and D. Serero. We want to thank them warmly. We wish also to thank M.E. Cates, J. Duran, G. Grest, A. Kamenev, E. Kolb, J.M. Luck, G. Ovarlez, Y. Roichman, J.N. Roux, D.G. Schaeffer, J.E.S. Socolar, L. Vanel and J.P. Wittmer for very useful discussions.

References

[1] J. Šmíd, J. Novosad, in: Proc. Powtech. Conference, 1981, Ind. Chem. Eng. Symp., Vol. 63, 1981, D3V 1.
[2] R. Brockbank, J.M. Huntley, R.C. Ball, J. Phys. (France) II 7 (1997) 1521.
[3] S.B. Savage, in: H.J. Herrmann, J.P. Hovi, S. Luding (Eds.), Physics of Dry Granular Media, NATO ASI, Vol. 25, 1997.
[4] L. Vanel, D.W. Howell, D. Clark, R.P. Behringer, E. Clément, Phys. Rev. E 60 (1999) R5040.
[5] P.-G. de Gennes, Physica A 261 (1998) 293.
[6] P.-G. de Gennes, Rev. Mod. Phys. 71 (1999) S374.
[7] J. Geng, E. Longhi, R.P. Behringer, D.W. Howell, Memory in 2D heap experiments, cond-mat/0109289.
[8] P. Dantu, Ann. Ponts Chaussées 4 (1967) 144.
[9] G. Josselin de Jong, A. Verruijt, Cah. Groupe Fr. Rheol. 2 (1969) 73.
[10] F. Calvetti, G. Combe, J. Lanier, Mech. Coh. Frict. Mat. 2 (1997) 121.
[11] F. Radjai, S. Roux, in: Kishino (Ed.), Proc. Meeting 'Powders and Grains', Balkema, Lisse, 2001, p. 21.
[12] F. Radjai, D.E. Wolf, M. Jean, J.J. Moreau, Phys. Rev. Lett. 80 (1998) 61.

[13] D. Mueth, H. Jaeger, S. Nagel, Phys. Rev. E 57 (1998) 3164.
[14] D.M. Wood, Soil Behaviour and Critical State Soil Mechanics, Cambridge University Press, Cambridge, 1990.
[15] G. Combe, J.-N. Roux, Phys. Rev. Lett. 85 (2000) 3628.
[16] J.-P. Bouchaud, M.E. Cates, P. Claudin, J. Phys. (France) I 5 (1995) 639.
[17] J.P. Wittmer, P. Claudin, M.E. Cates, J.-P. Bouchaud, Nature 382 (1996) 336.
[18] J.P. Wittmer, P. Claudin, M.E. Cates, J. Phys. (France) I 7 (1997) 39.
[19] J.-P. Bouchaud, P. Claudin, M.E. Cates, J.P. Wittmer, in: H.J. Herrmann, J.P. Hovi, S. Luding (Eds.), Physics of Dry Granular Media, NATO ASI, Vol. 97, 1997.
[20] P. Claudin, Ann. Phys. 24 (1999) 1.
[21] R.M. Nedderman, Statics and Kinematics of Granular Materials, Cambridge University Press, 1992.
[22] P. Claudin, J.-P. Bouchaud, M.E. Cates, J.P. Wittmer, Phys. Rev. E 57 (1998) 4441.
[23] L. Vanel, P. Claudin, J.-P. Bouchaud, M.E. Cates, E. Clément, J.P. Wittmer, Phys. Rev. Lett. 84 (2000) 1439.
[24] M.E. Cates, J.P. Wittmer, J.-P. Bouchaud, P. Claudin, Phys. Rev. Lett. 81 (1998) 1841.
[25] J.-N. Roux, Phys. Rev. E 61 (2000) 6802.
[26] C.F. Moukarzel, Phys. Rev. Lett. 81 (1998) 1634.
[27] S.F. Edwards, Physica A 249 (1998) 226.
[28] S.F. Edwards, D.V. Grinev, Phys. Rev. Lett. 82 (1999) 5397.
[29] V. Tkachenko, T.A. Witten, Phys. Rev. E 60 (1999) 687.
[30] V. Tkachenko, T.A. Witten, Phys. Rev. E 62 (2000) 2510.
[31] C.-h. Liu, S.R. Nagel, D.A. Schecter, S.N. Coppersmith, S. Majumdar, O. Narayan, T.A. Witten, Science 269 (1995) 513.
[32] S.N. Coppersmith, C.-h. Liu, S. Majumdar, O. Narayan, T.A. Witten, Phys. Rev. E 53 (1996) 4673.
[33] G. Reydellet, E. Clément, Phys. Rev. Lett. 86 (2001) 3308.
[34] J. Geng, D. Howell, E. Longhi, R.P. Behringer, G. Reydellet, L. Vanel, E. Clément, S. Luding, Phys. Rev. Lett. 87 (2001) 035506.
[35] N. Mueggenburg, H. Jaeger, S. Nagel, in preparation.
[36] M. da Silva, J. Rajchenbach, Nature 406 (2000) 70.
[37] J.-J. Moreau, in: Proc. Colloque 'Physique et mécanique des matériaux granulaires', Champs-sur-Marne, France, 2000, p. 199.
[38] S. Bernard-Bernardet, Sur la statique des empilements granulaires, Rapport de stage, École Centrale Paris, Chatenay Malabry, 2001;
D. Bonamy, PhD thesis, in preparation.
[39] D.A. Head, A.V. Tkachenko, T.A. Witten, Robust propagation direction of stresses in a minimal granular packing, Eur. Phys. J. E 6 (2001) 99.
[40] C. Eloy, E. Clément, J. Phys. I 7 (1997) 1541.
[41] L. Breton, P. Claudin, E. Clément, J.-D. Zucker, in preparation.
[42] C. Goldenberg, I. Goldhirsch, Force chains, microelasticity and macroelasticity, cond-mat/0108297.
[43] D. Serero, G. Reydellet, P. Claudin, E. Clément, D. Levine, Stress response function of a granular layer: quantitative comparison between experiments and isotropic elasticity, cond-mat/0107626.
[44] J. Garnier, Tassement et contraintes. Influence de la rigidité de la fondation et de l'anisotropie du massif, PhD thesis, Université de Grenoble, 1973.
[45] E. Clément, G. Reydellet, L. Vanel, D.W. Howell, J. Geng, R.P. Behringer, in: XIIIth Int. Cong. on Rheology, Cambridge, UK, Vol. 2, 2000, p. 426.
[46] J.-P. Bouchaud, P. Claudin, D. Levine, M. Otto, Eur. Phys. J. E 4 (2001) 451.
[47] L. Landau, E. Lifshitz, Elasticity theory, Pergamon, New York, 1986.
[48] K.L. Johnson, Contact Mechanics, Cambridge University Press, Cambridge, 1985.
[49] M.E. Cates, J.P. Wittmer, J.-P. Bouchaud, P. Claudin, Phil. Trans. Roy. Soc. London A 356 (1998) 2535.
[50] M.C.W. van Rossum, Th.M. Nieuwenhuizen, Rev. Mod. Phys. 71 (1999) 313.
[51] Y. Roichman, D. Levine, Scattering force chains: propagating stress in granular matter, preprint.
[52] M. Otto, J.-P. Bouchaud, P. Claudin, I.E.S. Socolar, in preparation.
[53] I.E.S. Socolar, D.G. Schaeffes, P. Claudin, cond-mat/0201242.